Acousto-optically tunable lithium niobate photonic crystal

Nadège Courjal,[a] Sarah Benchabane, Jean Dahdah, Gwenn Ulliac, Yannick Gruson, and Vincent Laude
Institut FEMTO-ST, Université de Franche-Comté, CNRS, 32 Avenue de l'Observatoire, F-25044 Besançon Cedex, France

(Received 5 December 2009; accepted 2 March 2010; published online 29 March 2010)

We report on an active two-dimensional lithium niobate photonic crystal (PhC) driven by stationary Rayleigh surface acoustic waves. The configuration relies on two interdigital transducers that modulate the refractive index through the acousto-optical effect. Highly efficient, compact acousto-optical PhCs with an active length of only 13 μm and a driving electrical power of 20 mW have been fabricated and characterized. Experiments show that an enhancement factor of the elasto-optical interaction of the order of 61 is obtained thanks to slow light effects in the PhC. © *2010 American Institute of Physics*. [doi:10.1063/1.3374886]

Photonic crystals offer a unique means of controlling light propagation at the wavelength scale. Their intrinsic capability to tailor the dispersion properties of light positions them as very powerful tools for the implementation of complex integrated optical functionalities. If the focus has initially been set on the realization of passive devices, the possibility to fabricate these photonic crystals (PhCs) on materials that are strongly sensitive to external stimuli has opened the way toward the development of tunable optical components. Different approaches have already been reported, relying on the use of electro-optical,[1,2] magneto-optical,[3] carrier injection,[4] or thermo-optical[5] modulation. Another versatile way to control the refractive index profile of the propagation medium is to make use of elastic waves. Acousto-optical devices have been widely used in their bulk configuration for instance for acousto-optical tunable filtering of laser sources or for pulse shaping in ultrashort lasers.[6] In integrated optics, most of the reported solutions rely on the use of surface acoustic waves (SAW) that can be easily generated atop a piezoelectric surface.[7] Their use however remains to date limited by their relatively low efficiency. There is hence a need for integrated device geometries allowing for an enhanced coupling between optical and elastic waves. In PhC-based solutions, slow light effects at the band gap edges allow for an increase in the interaction time and therefore in the effective interaction strength between the optical field and any external field applied to the medium. It has, for example, been shown that an enhancement factor of 312 times can be obtained in the case of an electro-optical modulation of an optical signal going through a two-dimensional (2D) PhC.[2] In this paper, we investigate the acousto-optical counterpart of such an effect. Up to now, acousto-optical control of PhCs has mostly been investigated for one-dimensional structures, as in semiconductor-based PhCs.[8–10] Here, we focus on a fully integrated configuration exploiting SAWs and 2D-PhCs written on optical waveguides. The developments are performed on a lithium niobate ($LiNbO_3$) substrate in view of exploiting its strong acousto-optical and piezoelectric coefficients.

The proposed device is schematically depicted in Fig. 1. It consists of a square lattice PhC integrated on a graded-index optical waveguide for transverse electric (TE) waves and surrounded by a pair of interdigital transducers (IDTs). Each IDT generates a Rayleigh SAW that propagates along the Z-axis of the $LiNbO_3$ crystal. The PhC was initially designed to have one of its spectral gap edge at 1500 nm for TE-polarized waves. This configuration offers the ability to control the output intensity; any external effect applied to the crystal and affecting the material refractive index will result in a shift in the band edge and hence in a modulation of the output optical signal. In this particular case, the strain and the piezoelectric field accompanying the acoustic wave propagation are expected to induce, respectively, an elasto- and an electro-optical modification of the refractive index. These contributions cause a change in the optical and structural properties of the PhC, provoking a shift in the spectral position of the photonic gap in the transmission response.

To increase the acousto-optical interaction strength, the geometrical properties of the fabricated PhC were initially

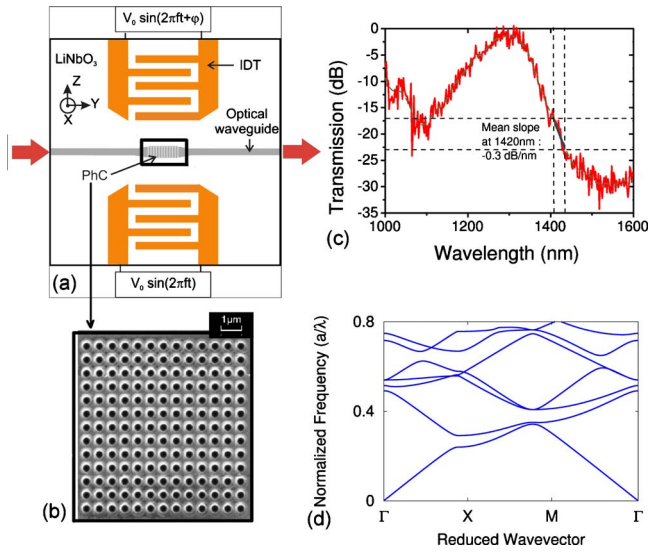

FIG. 1. (Color online) (a) Schematics of the acousto-optic modulators. (b) Scanning electron microscope image of the fabricated square lattice air/$LiNbO_3$ PhC. Pitch a=825 nm, diameter d=412 nm. (c) Measured optical transmission through the PhC (solid red line). Results obtained by normalizing the optical intensity transmitted through the nanostructured waveguide with the intensity through a single waveguide realized in the same conditions without any PhC. The dashed green line is the experimental result filtered using a low pass filter. (d) Corresponding band structure.

[a]Electronic mail: nadege.bodin@univ-fcomte.fr.

chosen to compensate for the small length of the active section by increasing the interaction time and enhancing the optical field within the PhC. By using plane wave expansion calculations performed using the RSOFT BANDSOLVE™ software, we have determined that a good compromise can be reached between low group velocity and low radiation losses if the PhC is made of a square array of air holes with a diameter to pitch ratio d/a equals to 0.5. Under these conditions, the dispersion relation exhibits a flat band in the ΓX direction, as seen in Fig. 1(d). The group velocity was then deduced from the slope of this fourth band and estimated to be around $0.024c$, i.e., 21 times slower than the group velocity in a regular straight graded-index waveguide. This band lies at a normalized frequency $a/\lambda=0.55$, where λ is the wavelength, hence imposing a period $a=825$ nm for operation at a wavelength of 1500 nm.

The PhC was fabricated on a 0.5 mm thick X-cut $LiNbO_3$ wafer. The optical graded-index waveguide was obtained through annealed proton exchange which, in the case of X-cut $LiNbO_3$, induces a guiding of the TE-polarized wave only. Proton-exchange was first achieved through a SiO_2 mask in benzoic acid at 180 °C for 2 h. The process was followed by an annealing of the obtained step-index optical waveguide at 333 °C for 4 h. With such experimental parameters, the optical core of the TE-polarized guided mode is estimated to be at 0.9 μm below the surface. The PhC itself was written on the waveguide by focused ion beam milling, as described in Ref. 11. The optical spectrum through the PhC was measured with a supercontinuum source and an Optical Spectrum Analyzer (Anritsu MS9710A) as described in Ref. 2. The resulting normalized transmission through the PhC is displayed in Fig. 1(c); it showed a gap between 1300 and 1750 nm and an extinction ratio of −30 dB between the maximum output intensity at 1300 nm and the minimum output intensity at 1500 nm. The small peaks that can be seen in the measured transmission response [see for example the one at 1400 nm in Fig. 1(c)] are assumed to be due to a Fabry–Perot effect between the PhC structure and the output of the waveguide. A smoothing of the transmission response using a low-pass filter was then performed in order to eliminate this contribution and evaluate the mean slope between 1410 and 1430 nm. The smoothed transmission response is represented with a dashed green line in Fig. 1(c) and exhibits a mean slope value of -0.3 dB $nm^{-1} \pm 1$ dB nm^{-1} at the operating wavelength of 1420 nm.

The two IDTs were subsequently fabricated by optical lithography and lift-off of a 200 nm thick evaporated aluminum layer. The transducers are identical, with an acoustic aperture of 400 μm and a period $p=9$ μm. The corresponding acoustic wavelength of 18 μm is then much larger than the optical waveguide width $w=5.5$ μm. This feature helps ensuring a constant amplitude of the acoustic wave across the PhC width. The overall electrical configuration was studied to reduce capacitive effects. The IDTs were then wire bonded to a printed circuit board designed to ensure impedance matching. Electrical excitation was achieved thanks to a single input electrical signal splitted and phaseshifted.

The SAWs are therefore generated with identical amplitudes and frequencies but with opposite directions of propagation. The resulting acoustic wave is then expected to exhibit an amplitude twice as large as the one obtained with a single IDT. The position of its maxima can be adjusted by changing the phase between the electric signals applied on each transducer. The resulting electrical transmission response S_{12} through the IDTs was measured with a network analyzer (Rhode & Schwarz ZVRC) and is reported with a solid black line in Fig. 2. The resonance frequency lies around 191.3 MHz, and the maximum of transmission through the connected IDTs was measured to be −7 dB, meaning that 44% of the electrical input power is converted into acoustic power at the resonance frequency.

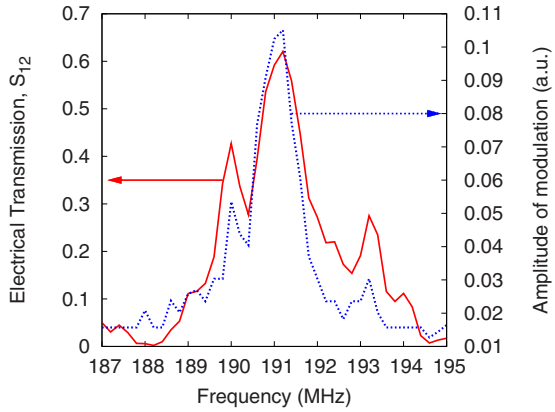

FIG. 2. (Color online) Amplitude of the optical intensity modulation (dashed blue line) in comparison with electric transmission s_{21} through the IDTs (solid red line).

Acousto-optical characterizations were then performed with a distributed feedback laser diode emitting at a wavelength of 1420 nm. The laser light was injected into the optical waveguide hosting the PhC. A power of 13 dBm at 191.3 MHz was here again applied at the entrance of the delay line, and the output voltage measured at the entrance of each IDT can be visualized in Fig. 3(a). As expected, the maximum of intensity modulation was obtained for an emission in phase and is reported in Fig. 3(b). The overall extinction ratio is around −5 dB. For a fixed delay between the two IDTs, the amplitude of modulation is maximum at the IDT resonance frequency and decreases when trailing away from it, as can be seen on the dashed line of Fig. 2. These results confirm that the acousto-optical effect predominates over pure electro-optical or thermo-optical effects, which are frequency independent. A contribution of the electro-optical effect can nevertheless be observed. Indeed, a residual modu-

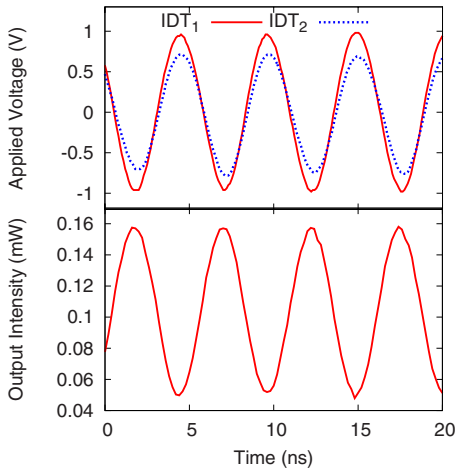

FIG. 3. (Color online) Modulation at 191.2 MHz. (a) Applied voltages on the two IDTs. (b) Resulting amplitude of the optical intensity modulation.

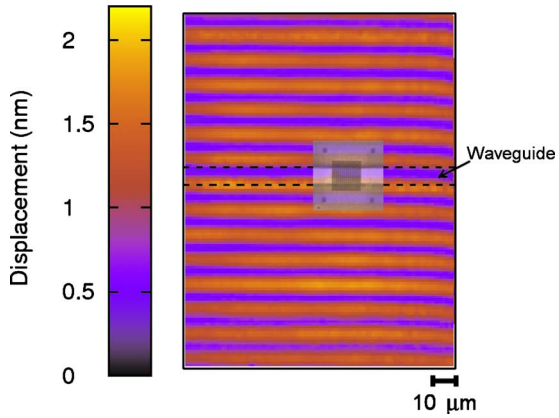

FIG. 4. (Color online) (a) Modulus of the vertical displacement field between the two IDTs measured using a laser heterodyne interferometer. A microscope image of the PhC and the optical waveguide is superimposed on the displacement image to show their actual position.

lation was measured far from the resonance, where the acousto-optical coupling is negligible (dashed curve of Fig. 2, i.e., at frequencies lower than 188 MHz or higher than 194 MHz). This residual modulation may be explained by the difference in amplitude between the signals applied to the IDTs. It can be seen in Fig. 3(b) that the signal applied to the first IDT is 0.23 V lower than the signal applied to the second one. This difference in amplitude generates an electrical field between the IDTs that does not depend on frequency. Previous works report that the electro-optically induced wavelength shift for the very same PhC structure is of 5 nm V^{-1},[2] resulting here in a shift of 1.15 nm and hence in a (0.35 ± 0.11) dB variation in the output intensity. This electro-optical contribution to intensity modulation should disappear with the use of a symmetric electrical splitter ensuring two strictly identical output voltages. Thus, an improvement of (0.35 ± 0.11) dB of the extinction ratio should be achieved. The frequency shift imputable to the acousto-optical modulation, corresponds to an extinction ratio of (5.4 ± 0.1) dB, hence resulting in a wavelength shift of (18 ± 6) nm as deduced from the mean slope value at 1420 nm measured on the transmission response. This change in wavelength can be directly translated in a variation in the refractive index using the simple relationship $\Delta\lambda = \lambda \cdot \Delta n / n$ where $n = 2.143$ is the effective refractive index. The obtained index change is therefore as high as $(2.5 \pm 0.8) \times 10^{-2}$.

The actual refractive index induced by the surface wave in the homogeneous medium was then worked out independently from measurements of the elastic displacement field. A scanning heterodyne laser interferometer[12] was used to characterize the displacement field over a scan area of 100×150 μm^2 encompassing the PhC, with a lateral scanning step of 1 μm. The maximum amplitude was obtained for devices emitting in phase and the corresponding scanned amplitude field is reported in Fig. 4. The amplitude data were then averaged in the y direction to retrieve the vibration amplitude. For an applied electrical input power of 13 dBm (before splitting) at 191.3 MHz, the measured vibration amplitude is of about 1.2 nm. The corresponding refractive index change was eventually calculated following Ref. 13. The so-called indirect photoelastic effect, linked to the electro-optical contribution caused by the piezolectric field carried by the propagating elastic wave,[14] was in addition taken into account, and the total refractive index change was then evaluated to be around 4.4×10^{-4}. The effective refractive index variation as felt by the PhC structure is then 61 times higher than the actual index change. Much similarly to what was observed with the electro-optical effect in Ref. 2, slow light phenomena linked to the dispersion properties of the PhC allows for a significant enhancement of the elasto-optical interaction, hence allowing for highly compact and efficient devices.

As a conclusion, we have demonstrated the feasibility of an acousto-optical micromodulator on $LiNbO_3$ substrates with an active length of only 13 μm. Modulation with an extinctio ratio of 5 dB was achieved at 200 MHz for a driving power of 20 mW only. The low driving power required demonstrates the influence of the photonic structure which increases the overall device efficiency by a factor of 61. Higher extinction ratios along with increased efficiency can be expected from an improvement of the PhC fabrication process (increase in side wall verticality) or by ensuring a joint confinement of sound and light. The obtained results open appealing perspectives for the realization of miniature dynamic optical circuits.

The authors gratefully acknowledge O. Gaiffe for his help with elastic displacement field measurements.

[1] M. Roussey, M. Bernal, N. Courjal, and F. Baida, Appl. Phys. Lett. **87**, 241101 (2005).
[2] M. Roussey, M.-P. Bernal, N. Courjal, D. V. Labeke, F. I. Baida, and R. Salut, Appl. Phys. Lett. **89**, 241110 (2006).
[3] M. Diwekar, V. Kamaev, J. Shi, and Z. V. Vardeny, Appl. Phys. Lett. **84**, 3112 (2004).
[4] L. Gu, W. Jiang, X. Chen, L. Wang, and R. T. Chen, Appl. Phys. Lett. **90**, 071105 (2007).
[5] E. A. Camargo, H. M. H. Chong, and R. M. D. L. Rue, Opt. Express **12**, 588 (2004).
[6] F. Verluise, V. Laude, Z. Cheng, C. Spielmann, and P. Tournois, Opt. Lett. **25**, 575 (2000).
[7] R. M. White and F. W. Voltmer, Appl. Phys. Lett. **7**, 314 (1965).
[8] P. V. Santos, J. Appl. Phys. **89**, 5060 (2001).
[9] M. M. de Lima, Jr., R. Hey, and P. V. Santos, Appl. Phys. Lett. **83**, 2997 (2003).
[10] P. D. Batista, B. Drescher, W. Seidel, J. Rudolph, S. Jiao, and P. V. Santos, Appl. Phys. Lett. **92**, 133502 (2008).
[11] F. Lacour, N. Courjal, M.-P. Bernal, A. Sabac, C. Bainier, and M. Spajer, Opt. Mater. (Amsterdam, Neth.) **27**, 1421 (2005).
[12] P. Vairac and B. Cretin, Opt. Commun. **132**, 19 (1996).
[13] D. Gérard, V. Laude, B. Sadani, A. Khelif, D. V. Labeke, and B. Guizal, Phys. Rev. B **76**, 235427 (2007).
[14] R. V. Schmidt, IEEE Trans. Sonics Ultrason. **23**, 22 (1976).